

Dielectric properties of metallic alloy FeCoZr-dielectric ceramic PZT nanostructures prepared by ion sputtering in vacuum conditions

O Boiko

Electrical Engineering and Computer Science Faculty, Lublin University of Technology, 38A Nadbystrzycka Street, 20-618 Lublin, Poland

E-mail: oleksandr.boiko@pollub.edu.pl

Abstract. The main objective of the research was investigation of dielectric properties of $(\text{FeCoZr})_x(\text{PZT})_{(100-x)}$ granular nanocomposites and determination the influence of isochronous annealing in temperatures of 398 K-573 K on them. The impedance spectroscopy methodology was used. The measurements of electrical parameters, such as: phase shift angle φ , dielectric loss factor $\text{tg}\delta$, capacity C and conductivity σ of $(\text{FeCoZr})_x(\text{PZT})_{(100-x)}$ nanocomposites have been performed. Frequency dependencies of these parameters were obtained for the ambient temperature range 98 K-373 K for the frequencies ranging from 50 Hz to 10^5 Hz. It was established, that the conductivity σ of the tested materials before the percolation threshold demonstrates non-linear dependence on frequency. Furthermore, it increases when the ambient temperature is increasing, which indicates a dielectric type of the material. The two types of electrical conduction: capacitive (phase shift angle φ takes negative values) and inductive (φ takes positive values) have been observed. It was concluded that the hopping conductivity dominated in the nanocomposites. Voltage and current resonances phenomena are observed in the materials. The isochronous annealing intensifies the dielectric properties of $(\text{FeCoZr})_x(\text{PZT})_{(100-x)}$ nanocomposites.

1. Introduction

Ultralight soft structures with high temperature capability are a very important class of materials with very high implementation potential [1,2]. High values of Curie temperatures for iron (1043 K) and cobalt (1388 K) formed the basis for the development and broadening of the research spectrum of magneto-soft materials containing these elements or their alloys [3,4]. However, thin films FeCo demonstrate high values of coercivity H_c (100-200 Oe) and magneto-crystalline anisotropy, which makes it difficult to find some potential applications. One of the solutions is adding (alloying) some additional metalloid component (“semi-metal”) to the structure of FeCo alloy. The examples of such materials are: CoFeZr [5], CoFeB [6], CoFeNi [7], CoFeAl [8] etc.

Studies of electro-magnetic properties carried out over the last twenty years have shown that ferromagnetic materials in combination with piezo or ferroelectric components form structures, properties of which are changing under the influence of both electric and magnetic fields [9,10]. A frequently used ferroelectric for this purpose is Lead Zirconate Titanate PbZrTiO_3 , which is a typical material with piezoelectric properties [11,12]. It belongs to the group of ceramic due to the structure and manufacturing methods.



The materials been tested in the present paper are nanostructures contains FeCoZr ferromagnetic alloy nanoparticles randomly arranged in Lead Zirconate Titanate ferroelectric matrix PbZrTiO_3 (abbreviated as PZT). The dielectric matrix of PZT was chosen for samples production due to its specific features: it's less corrosion-resistant matrix than alumina (according to previous investigations of $(\text{FeCoZr})_x(\text{Al}_2\text{O}_3)_{(100-x)}$ nanocomposites) [13], and having crystalline structure it demonstrate ferroelectric or piezoelectric properties [14], which broaden the spectrum of its investigations. Furthermore, $(\text{FeCoZr})_x(\text{PZT})_{(100-x)}$ nanofilms are interesting structures to study percolation and resonant phenomena [15], hopping conductivity and relaxation mechanisms [16] in bulk materials.

The paper contains new experience in describing of dielectric properties of novel materials with use of dielectric spectroscopy method. Furthermore, the article presents a big number of nanocomposites potential applications due to demonstrated properties and original information about modelling and experimental results.

2. Experimental

The main objective of the research – granular nanomaterials of $(\text{FeCoZr})_x(\text{PZT})_{(100-x)}$, where x – metallic concentration (at.%), were produced using ion sputtering technique in a vacuum chamber. The sputtered beam during the process of nanocomposites synthesis included mixture of argon Ar and oxygen O_2 ions with its partial pressures of $P_{\text{Ar}} = 7.4 \times 10^{-2}$ Pa and $P_{\text{O}_2} = 3.0 \times 10^{-3}$ Pa, respectively. Sputtering target consisted of the metallic alloy FeCoZr plate and ferroelectric ceramic PZT ribbons (with different distances between them) attached to it, which allowed to obtain series from 11 nanocomposite samples with various ratios of metallic and dielectric phases x ranging from 29.0 at.% to 90.0 at.% during one production cycle. Glass-ceramic substrates were used for nanolayers deposition at temperature of 373 K. All of the details related to films production process are described in [15]. The chemical compositions of the $(\text{FeCoZr})_x(\text{PZT})_{(100-x)}$ nanolayers were investigated by using of energy-dispersive X-ray spectroscopy and Rutherford Backscattering technique. Samples thicknesses were verified by SEM with accuracy of approx. 3 % and got values from the range of 0.4 μm -2 μm . To examine the structure and phase state of the nanocomposites Mössbauer spectroscopy was used. All of the details related to structure and chemical composition investigations of tested nanomaterials are described in [17,18].

Table 1. Samples specifications and parameters.

x (at.%)	h (μm)	a (cm)	b (cm)	R ($\text{M}\Omega$)	σ ($\text{k}\Omega \cdot \text{cm}$) ⁻¹	C (F)	$\text{tg}\delta$ (a.u.)
29.0	0.4016	0.46	0.20	168.00	0.137	2.76E-12	6.87
49.8	1.3067	0.20	0.20	71.54	0.321	6.18E-12	7.20
64.4	1.0899	0.46	0.21	1.79	127.362	7.68E-09	2.32
80.0	1.5692	0.46	0.20	0.15	977.304	1.1E-07	1.94
90.0	0.8400	0.47	0.20	2.97	49.321	1.09E-08	0.99

Some specifications related to samples dimensions and electrical parameters at room temperature ($f = 50$ Hz) are presented in table 1. The table includes: a – length, b – width, h – thickness, R – resistance, σ – conductivity, C – capacity and $\text{tg}\delta$ – loss factor. In order to investigate the dielectric properties of tested materials the impedance spectroscopy was used. Measurements of electrical parameters (phase shift angle φ , conductivity σ , capacity C and loss coefficient $\text{tg}\delta$) have been conducted using experimental station described in [19]. Frequency dependencies of $\varphi(f)$, $\sigma(f)$, $C(f)$ and $\text{tg}\delta(f)$ have been obtained for ambient temperatures range of $98 \text{ K} \leq T_p \leq 373 \text{ K}$ for frequencies of 50 Hz to 10^5 Hz. To determine the impact of thermal treatment on dielectric properties $(\text{FeCoZr})_x(\text{PZT})_{(100-x)}$ films were subjected to 15-min. isochronous annealing in tubular heater (air atmosphere) in temperatures of $398 \text{ K} \leq T_a \leq 573 \text{ K}$ with a step of 25 K. The publication presents the results of AC dielectric parameters measurements obtained for nanocomposites with $x_1 = 49.8$ at.% and $x_2 = 64.4$ at.% ratios.

3. Results and discussion

Figure 1 presents selected conductivity (case 1a) and phase shift angle (case 1b) versus frequency characteristics for a nanocomposite sample of $x_1 = 49.8$ at.%. The measurements have been performed directly after samples production. From the figure 1(a) can be observed that conductivity σ increases (two orders of magnitude) when measurement temperature increase. Such behaviour is typical for dielectric materials [20]. In this case the influence of temperature in conductivity in suitable temperature ranges can be described by the relationship:

$$\sigma = \sigma_0 \exp\left(-\frac{E_g}{2kT}\right) \quad (1)$$

where σ_0 – fixed value for each dielectric material, E_g – band gap energy, k – Boltzmann constant.

On the other hand, σ demonstrates a weak dependence on frequency. Figure 1(b) illustrates that phase angle φ takes negative values from approx. 0° to approx. -90° as the frequency f increases. This means, that the nanocomposite indicates capacitive type of current conduction. Capacitive properties of $(\text{FeCoZr})_x(\text{PZT})_{(100-x)}$ nanocomposites are described in [21]. The materials exhibit such kind of properties can find potential application in the industry as low-dimensional capacitors or nanosensors.

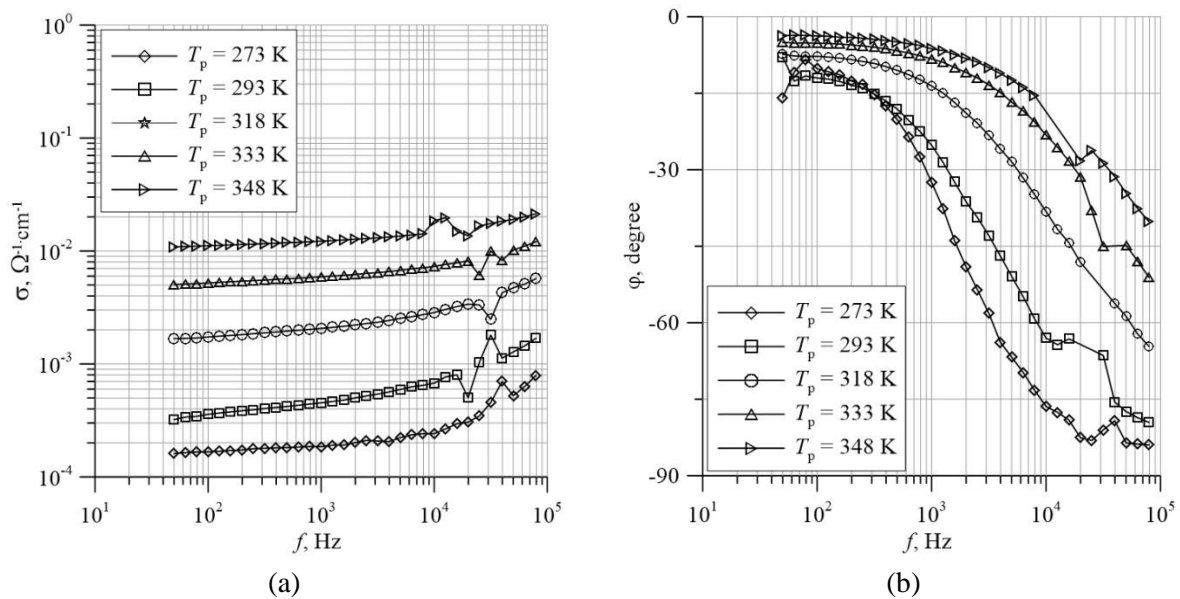


Figure 1. Frequency dependencies of: (a) conductivity σ and (b) phase shift angle φ of $(\text{FeCoZr})_{49.8}(\text{PZT})_{50.2}$ nanocomposite measured directly after preparing for selected ambient temperatures T_p .

To investigate the influence of isochronous annealing on dielectric properties $(\text{FeCoZr})_{49.8}(\text{PZT})_{50.2}$ sample was heated at temperature of $T_a = 523$ K. This time we can observe completely different situation, presented in figure 2. The materials conductivity σ at temperatures of $T_p < 318$ K exhibits nonlinear behaviour (figure 2(a)). Furthermore, we can notice the occurrence of its local minima for frequencies of f_{RP} . From figure 2(d) we can also observe minimal values of $\text{tg}\delta(f)$ dependencies at the same frequencies. It can be explained in the next way: at this situation f_{RP} is a resonant frequency and we can ascertain that the current resonant phenomenon appears in the material. The resonant frequency can be found using formula:

$$f_{\text{RP}} = \frac{1}{2\pi(L_p C_p)^{1/2}} \quad (2)$$

where L_p and C_p – inductance and capacitance in parallel circuit, (as shown in figure 3(a)). This electrical phenomenon are widely observed in electronics and can be presented using equivalent circuit diagram of parallel connection of RLC elements, as shown in figure 3(a). At this case, \underline{U} – voltage across the open terminals, current through the capacitor C_p equals the current through the inductor $L_p \rightarrow I_C = I_L$, but they are in opposite phases which means that the resulting current equals to the current through reactance $R_p \rightarrow I = I_R$. It should be admitted, that it is one of the rear cases when current resonant is observed with nonzero value of phase angle φ (in our case $\varphi = +90^\circ$, see figure 2(b)).

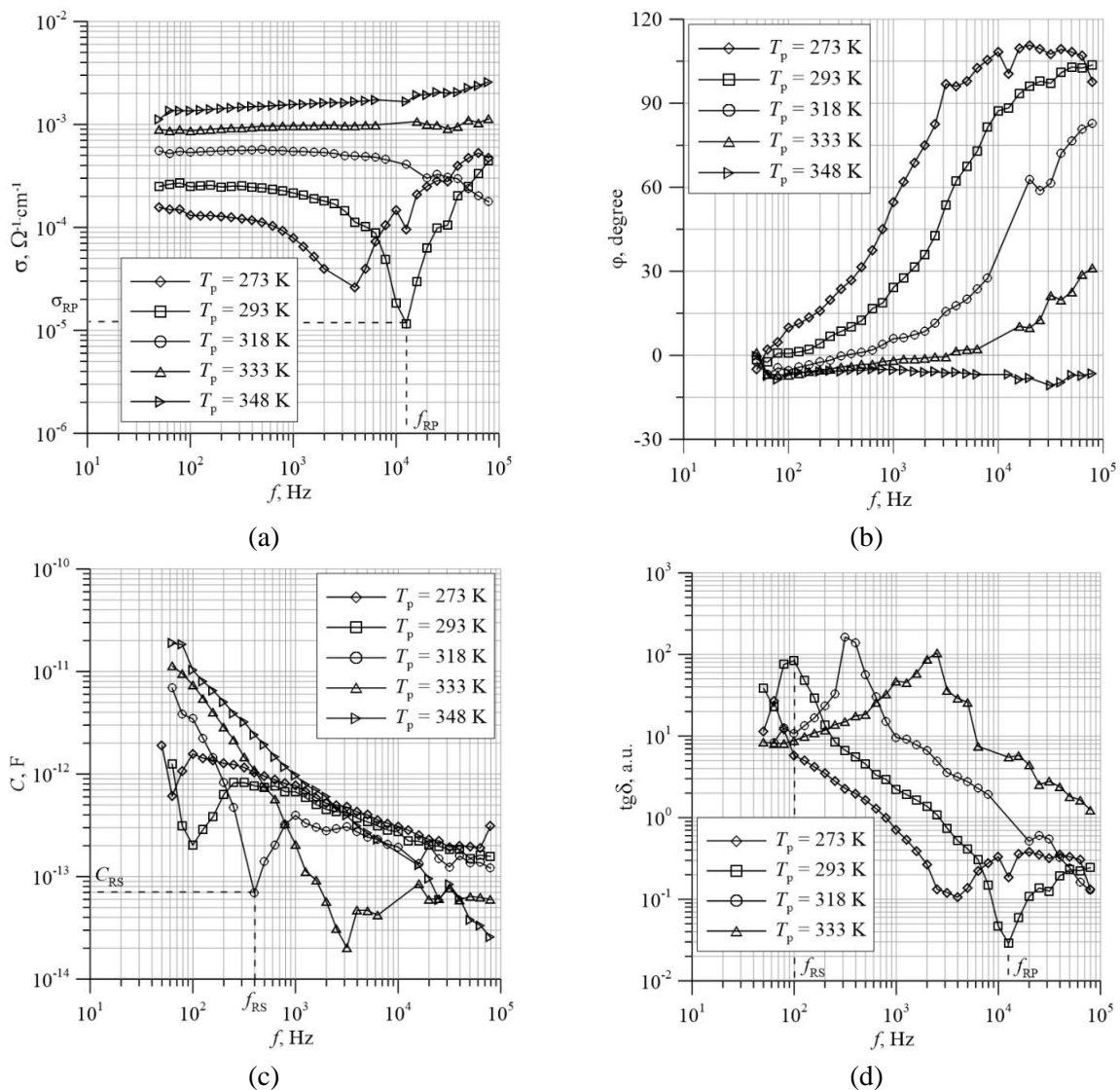


Figure 2. Frequency dependencies of: (a) conductivity σ , (b) phase shift angle φ , (c) capacity C and (d) loss coefficient $\text{tg} \delta$ of $(\text{FeCoZr})_{49.8}(\text{PZT})_{50.2}$ nanocomposite measured after 15-min. thermal treatment in temperature of $T_a = 523$ K.

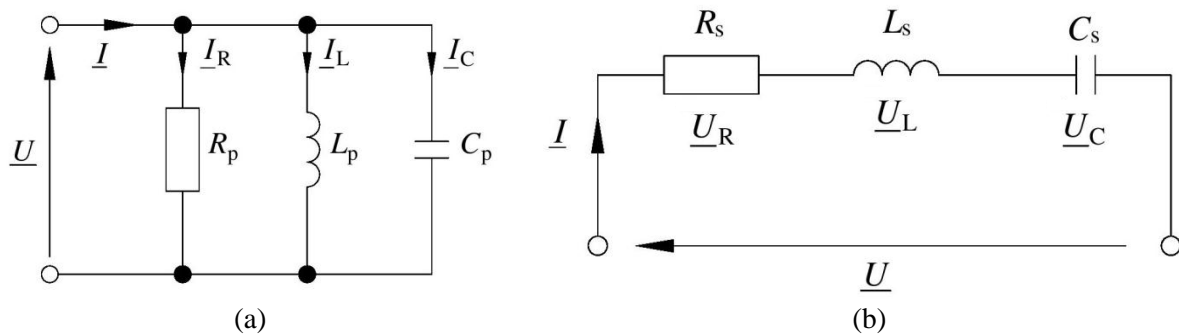


Figure 3. Equivalent circuit diagram of for both resonant cases: (a) current resonance: and (b) voltage resonance phenomena.

Figure 2(b) shows us positive values of phase shift angle φ for the temperatures of $T_p \leq 318$ K. The isochronous annealing in 523 K caused changes in the type of electrical conduction from capacitive to inductive. At this case, we can observe interesting electrical property of the nanocomposite, so-called non-coil inductance. Such sudden change in the conduction type can be related to the additional oxidation of metallic nanoparticles within ferroelectric volume which intensifies dielectric properties. Oxide shell around nanoparticle forms additional potential barrier which the charges should overcome to take part in electrical conduction [18]. Non-coil inductance means that nanocomposite sample, compared to conventional inductor, doesn't have a coil and a core from the material with magnetic properties. In case of $(\text{FeCoZr})_x(\text{PZT})_{(100-x)}$ nanolayers last can be replaced by FeCoZr nanoparticles because of its ferromagnetic nature.

Frequency dependence of capacity C is presented in figure 2(c). We can notice that, $C(f)$ for the temperatures $T_p \leq 318$ K demonstrates some minimal values at the frequencies f_{RS} . At the same frequencies $\text{tg}\delta$ characteristics take maximum values and phase shift angle achieves zero value. Such situation clearly indicates voltage resonance phenomenon in conventional RLC circuits, so-called series resonance. At this case current I is the same on each elements, the voltages $U = U_R$ and inductive reactance X_L and capacitive reactance X_C of a circuit are equal:

$$X_L = X_C \quad (3)$$

than

$$\omega_{RS} L_S = (\omega_{RS} C_S)^{-1} \quad (4)$$

Due to the fact that angular frequency $\omega_{RS} = 2\pi f_{RS}$, resonant frequency f_{RS} can be found as follows:

$$f_{RS} = \frac{1}{2\pi(L_S C_S)^{1/2}} \quad (5)$$

where L_S and C_S – inductance and capacitance in series circuit, (as shown in figure 3(b)).

Observation these phenomena indicates possible applications of $(\text{FeCoZr})_x(\text{PZT})_{(100-x)}$ nanofilms in electronics in radio transmitters, tuned circuits, filters, oscillators and other electrical devices working in wide frequency spectrum.

4. Hopping charge exchange in nanocomposites

Metal-dielectric nanocomposites with granular structure in a number of cases exhibit electrical conduction of hopping type [15]. It is related to the non-linear exponential dependence of conductivity on frequency. Same situation occurs in the case of FeCoZr-PZT nanocomposites below the percolation threshold as was established in [13] and is shown on figure 4(a). Figure 4(a) demonstrates conductivity versus frequency characteristics for nanocomposite sample with $x_2 = 64.4$ at.% subjected to thermal

treatment in tubular heater at temperature of $T_a = 573$ K. To examine the mechanism of electrical conduction of $(\text{FeCoZr})_x(\text{PZT})_{(100-x)}$ nanolayers the model of hopping conductance was used. The detailed description, main assumptions and its verification can be found in [13]. Moreover, some simulations of electrical parameters of tested materials were conducted in [16].

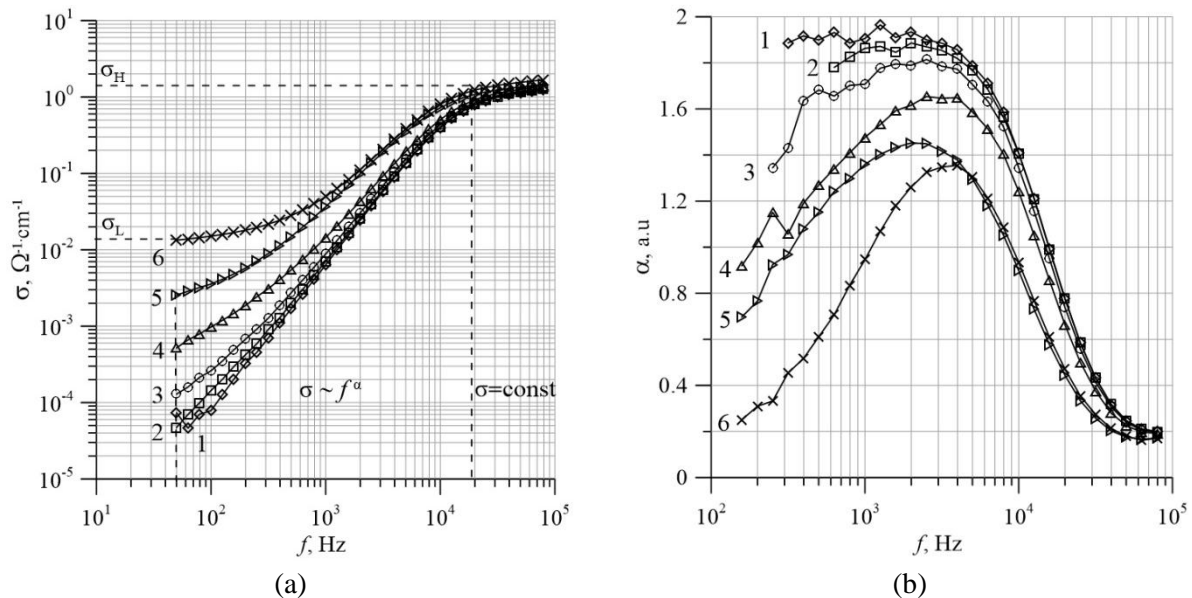


Figure 4. Frequency dependencies of: (a) conductivity σ and (b) frequency factor α of nanocomposites sample $x = 64.4$ at.% measured after 15-min. thermal treatment in temperature of $T_a = 573$ K for temperatures: 1 – 98 K, 2 – 153 K, 3 – 218 K, 4 – 273 K, 5 – 313 K, 6 – 373 K.

In the case of sample x_2 , the $\sigma(f, T_p)$ dependencies for nanocomposites in dielectric regime are characterized by a sigmoid-like shapes, displaying three frequency areas (curve 6 on figure 4(a)): low-frequency area where $\sigma_L \approx \text{const}$, medium frequencies with non-linear behaviour, high-frequency area with $\sigma_H \approx \text{const}$. From figures 2(a) (temperature range $T_p \leq 293$ K) and 4(a) (temperatures of 98 K-373 K) we can observe strong conductivity versus frequency dependence:

$$\sigma(f) \sim \sigma_0 f^{\alpha(p)} \quad (6)$$

where $\alpha(p)$ is the frequency coefficient dependent on probability of electrons hops p . Electrical conduction in the material is carrying out in a way of hopping charge exchange (on different distances) between the potential wells (FeCoZr nanoparticles). The probability of such hops p and the return hops $(1-p)$ can be described using following relation:

$$p = \frac{\sigma_L}{2\sigma_H} \quad (7)$$

In the case of tested samples parameter p takes values from 2×10^{-5} ($T_p = 98$ K) to 5×10^{-3} ($T_p = 373$ K). Frequency dependencies of exponent α are shown in figure 4(b). According to the model, α should take values from the range of $0 < \alpha < 2$ what we can notice in figure 4(b). The complex analyses of the results of electrical measurements contained in the section can be concluded that $(\text{FeCoZr})_x(\text{PZT})_{(100-x)}$ nanocomposites demonstrates hopping conductivity in alternating current at frequencies ranging from 50 Hz to 10^5 Hz.

5. Conclusions

AC electrical parameters measurements of $(\text{FeCoZr})_x(\text{PZT})_{(100-x)}$ nanolayers with $x_1 = 49.8$ at.% and $x_2 = 64.4$ at.% have been performed. The frequency and temperature dependencies of capacity C , conductivity σ , phase angle ϕ , loss coefficient $\text{tg}\delta$ and exponent α have been obtained. Dielectric properties of the materials measured directly after producing and subdued to thermal treatment at temperatures of 523 K and 573 K have been investigated. It was concluded that:

- Non-annealed nanolayer $(\text{FeCoZr})_{49.8}(\text{PZT})_{50.2}$ demonstrates dielectric type of conduction. Conductivity σ of the material is almost independent on frequency but shows temperature dependence, and phase shift angle ϕ takes negative values in whole frequency range;
- After the annealing of the sample in temperature of 523 K the materials character changes from capacitive to inductive due to the positive values of ϕ . Current and voltage resonances at resonant frequencies f_{RP}/f_{RS} and non-coil inductance phenomena in whole frequency range can be observed. Isochronous annealing intensifies the dielectric properties of the layer;
- Nanofilm $(\text{FeCoZr})_{64.4}(\text{PZT})_{35.6}$ annealed in temperature of 573 K demonstrates nonlinear exponential dependence of conductivity versus frequency. In both cases (figures 2(a) and 4(a)) the mechanism of charge carriers of the materials are defined as hopping conductivity;
- Potential applications of the tested materials in micro/nanoelectronics and electrical engineering have been considered.

References

- [1] Li X, Dong Y, Liu M, Chang C and Wang X M 2017 *J. Alloy. Compd.* **696** 1323-8
- [2] Yang B, Li X, Guo R and Yu R 2017 *Mater. Design* **121** 272-9
- [3] Hoque S M, Makineni S K, Pal A, Ayyub P and Chattopadhyay K 2015 *J. Alloy. Compd.* **620** 442-50
- [4] Le Graet C, Spenato D, Beaulieu N, Dekadjevi D T, Jay J-Ph, Pogossian S P, Warot-Fonrose B and Ben Youssef J B 2016 *EPL* **115** 17002
- [5] Zheng F, Ma Z, Gao H, Pan F C, Li S T, Cao J W, Bai J M and Wei F L 2017 *J. Electron. Mater.* **28** 17448-52
- [6] Wisniowski P, Dabek M, Wrona J, Cardoso S and Freitas P P 2017 *J. Appl. Phys.* **122** 213906
- [7] El Kammouni R, Kurlyandskaya G V, Vazquez M and Volchikov S O 2016 *Sensor. Actuat. A-Phys.* **248** 155-61
- [8] Wu D, Zhang Z, Li L, Zhang Z, Zhao H B, Wang J, Ma B and Jin Q Y 2015 *Sci. Rep.-UK* **5** 12352
- [9] Nayek C, Murugavel P, Kumar S D and Subramanian V 2015 *Appl. Phys. A-Mater.* **120** 615-22
- [10] Shimomura N, Sawada K, Nozaki T, Doi M and Sahashi M 2012 *Appl. Phys. Lett.* **101** 012403
- [11] Zhu D P, Jiang Q H and Li Y W 2017 *Mater. Res. Express* **4** 125705
- [12] Lu G P, Dong H T, Chen J G and Cheng J G 2017 *J. Sol-Gel Sci. Tech.* **82** 530-5
- [13] Koltunowicz T N, Zukowski P, Boiko O, Saad A, Fedotova J A, Fedotov A K, Larkin A V and Kasiuk J 2015 *J. Electron. Mater.* **44** 2260-8
- [14] Xiao M, Zhang Z B, Zhang W K and Zhang P 2017 *Appl. Phys. A-Mater.* **124** 8
- [15] Boiko O, Koltunowicz T N, Zukowski P, Fedotov A K and Larkin A V 2017 *Ceram. Int.* **43** 2511-6
- [16] Zukowski P, Koltunowicz T N, Boiko O, Bondariev V, Czarnacka K, Fedotova J A, Fedotov A K and Svito I A 2015 *Vacuum* **120** 37-43
- [17] Kasiuk J V, Fedotova J A, Marszalek M, Karczmarska A, Mitura-Nowak M, Kalinin Y E and Sitnikov A V 2012 *Solid State Phys.* **54** 178-84
- [18] Koltunowicz T N, Fedotova J A, Zhukowski P, Saad A, Fedotov A, Kasiuk J V and Larkin A V 2013 *J. Phys. D: Appl. Phys.* **46** 125304
- [19] Koltunowicz T N 2015 *J. Appl. Spectrosc.* **82** 653-8
- [20] Koltunowicz T N, Zukowski P, Czarnacka K, Boiko O, Fedotova J A and Kasiuk J V 2015 *J. Alloy. Compd.* **650** 262-7

- [21] Koltunowicz T N, Zukowski P, Boiko O, Czarnacka K, Bondariev V, Saad A, Larkin A V and Fedotov A K 2016 *J. Mater. Sci.-Mater. El.* **27** 1171-6